

Supplementary information

Radioactive hybrid semiconducting polymer nanoparticles for imaging-guided tri-modal therapy of breast cancer

Junhao Gu,^{‡a} Danling Cheng,^{‡a} Haiyan Li,^{‡b} Tao Yu,^a Zhenghe Zhang,^a Yue Liu,^a Xiaoying Wang,^{*c} Xia Lu^{*b} and Jingchao Li^{*a}

^a State Key Laboratory for Modification of Chemical Fibers and Polymer Materials, Shanghai Engineering Research Center of Nano-Biomaterials and Regenerative Medicine, College of Biological Science and Medical Engineering, Donghua University, Shanghai 201620, P. R. China

^b Department of Nuclear Medicine, Northern Jiangsu People's Hospital, Clinical Medical College, Yangzhou University, Yangzhou 225001, P. R. China

^c Office of Hospital Infection and Disease Control and Prevention, Shanghai General Hospital, Shanghai Jiao Tong University School of Medicine, Shanghai 200080, P. R. China

[‡] Contributed equally to this work.

*Corresponding authors:

goodwxyz@163.com (X. Wang); lxgf2222@163.com (X. Lu); jcli@dhu.edu.cn (J. Li)

Tabel S1. Hydrodynamic diameters of SPN_H at the different feeding weights of PCPDTBT, PFODBT and F127.

| Feeding weight of PCPDTBT, PFODBT and F127 | Hydrodynamic diameter (nm) |
|--|----------------------------|
| 1:1:20 | 110 ± 1.7 |
| 1:1:50 | 111.7 ± 5.0 |
| 1:1:100 | 119.5 ± 2.2 |
| 1:1:200 | 62.1 ± 1.5 |

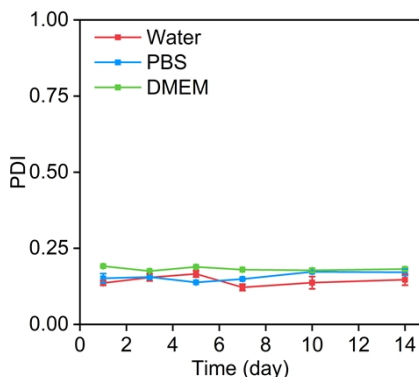


Fig. S1. PDI of SPN_H measured in different solutions (water, PBS and DMEM cell culture medium) at various days ($n = 5$).

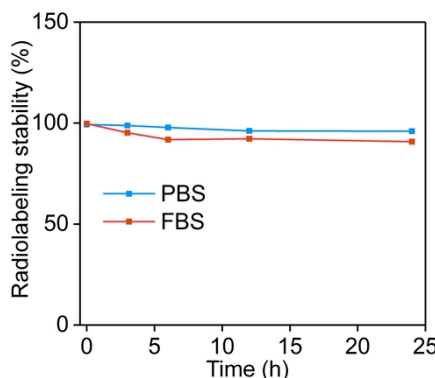


Fig. S2. Radiolabeling stability of SPN_H in different solution systems for various time ($n = 3$).

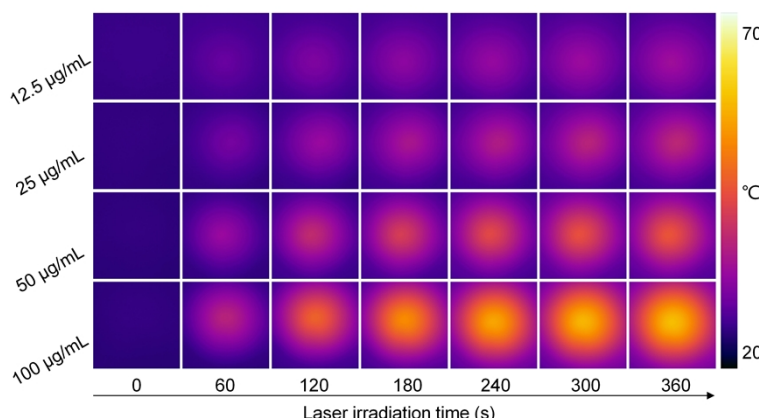


Fig. S3. Thermal images of aqueous solutions containing SPN_H at various SP concentrations (12.5, 25, 50 and 100 $\mu\text{g/mL}$) under 808 nm laser irradiation (1 W/cm^2) for 360 s.

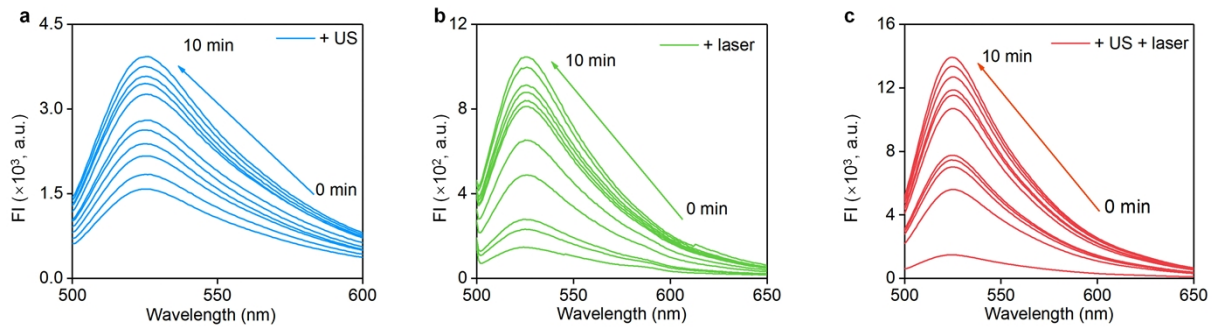


Fig. S4. Fluorescence intensities of SOSG solutions containing SPN_H under different treatments: (a) SPN_H + US, (b) SPN_H + laser, and (c) SPN_H + US + laser.

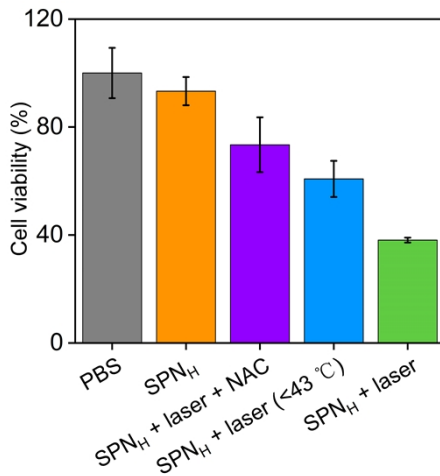


Fig. S5. Cell viability analysis of 4T1 cells in PBS, SPN_H, SPN_H + laser + NAC, SPN_H + laser (< 43 °C) and SPN_H + laser groups (n = 5).

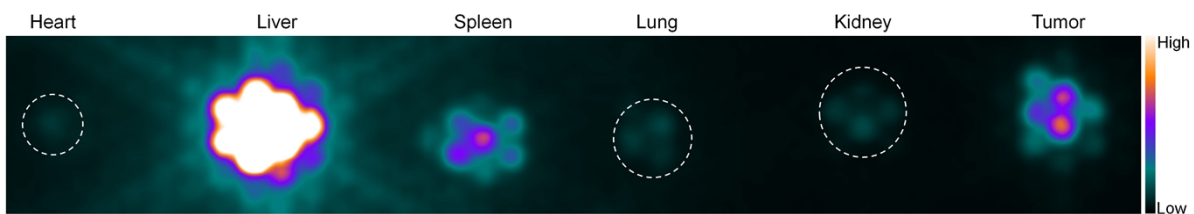


Fig. S6. Ex vivo SPECT imaging of heart, liver, spleen, lung, kidney and tumor separated from SPN_H-injected tumor-bearing mice.

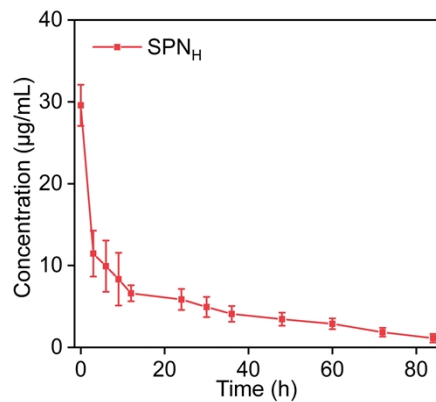


Fig. S7. Pharmacokinetic analysis of SPN_H in mice ($n = 3$).

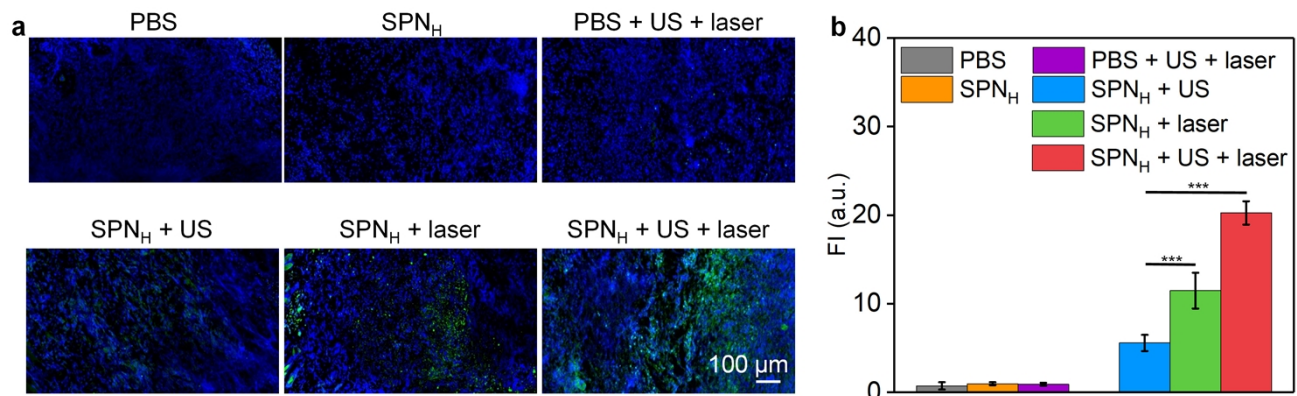


Fig. S8. (a) Fluorescence images of the produced ${}^1\text{O}_2$ in 4T1 subcutaneous tumors in each group. (b) Green fluorescence intensity (FI) of produced ${}^1\text{O}_2$ in 4T1 subcutaneous tumors ($n = 3$).

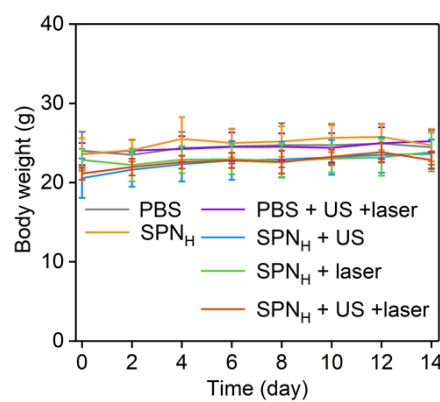


Fig. S9. The body weights of mice in various treatment groups ($n = 5$).

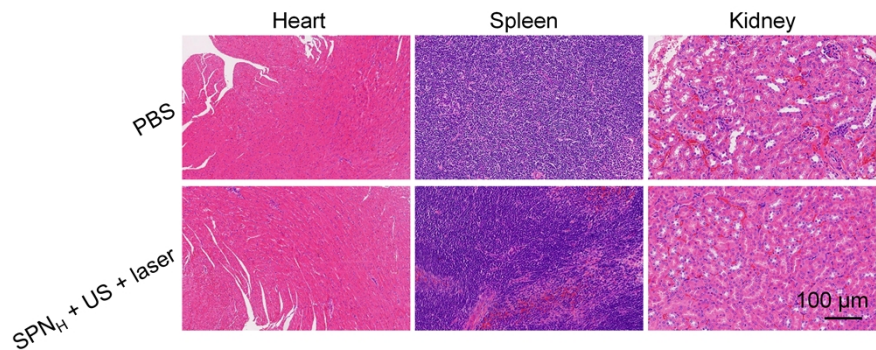


Fig. S10. H&E staining images of heart, spleen and kidney of mice in PBS and SPN_H + US + laser groups.